Human Brain Mapping

WILEY

RESEARCH ARTICLE OPEN ACCESS

Non-invasive Assessment of Cerebral Hemodynamics Using Resting-State Functional Magnetic Resonance Imaging in Multiple Sclerosis and Age-Related White Matter Lesions

Ahmed Khalil[1] | Susanna Asseyer[2,3,4] | Rebekka Rust[2,5] | Tanja Schmitz-Hübsch[2,3,4] | Jochen B. Fiebach[1] | Friedemann Paul[2,3] | Claudia Chien[2,3,4,6]

[1]Center for Stroke Research Berlin, Charité – Universitätsmedizin Berlin, Corporate Member of Freie Universität Berlin and Humboldt-Universität zu Berlin, Berlin, Germany | [2]Experimental and Clinical Research Center, a Cooperation Between the Max Delbrück Center for Molecular Medicine in the Helmholtz Association and the Charité – Universitätsmedizin Berlin, Berlin, Germany | [3]Max-Delbrück Center for Molecular Medicine in the Helmholtz Association, Berlin, Germany | [4]NeuroCure Clinical Research Center, Charité – Universitätsmedizin Berlin, Corporate Member of Freie Universität Berlin and Humboldt-Universität zu Berlin, Berlin, Germany | [5]Institute of Medical Immunology, Charité – Universitätsmedizin Berlin, Corporate Member of Freie Universität Berlin and Humboldt-Universität zu Berlin, Berlin, Germany | [6]Department of Psychiatry and Psychotherapy, Charité – Universitätsmedizin Berlin, Corporate Member of Freie Universität Berlin, Humboldt-Universität zu Berlin, Berlin, Germany

Correspondence: Ahmed Khalil (ahmed-abdelrahim.khalil@charite.de)

Received: 15 August 2024 | **Revised:** 31 October 2024 | **Accepted:** 4 November 2024

Funding: The authors received no specific funding for this work.

Keywords: microangiopathy | multiple sclerosis | perfusion | small vessel disease | white matter lesions

ABSTRACT

Perfusion changes in white matter (WM) lesions and normal-appearing brain regions play an important pathophysiological role in multiple sclerosis (MS). However, most perfusion imaging methods require exogenous contrast agents, the repeated use of which is discouraged. Using resting-state functional MRI (rs-fMRI), we aimed to investigate differences in perfusion between white matter lesions and normal-appearing brain regions in MS and healthy participants. A total of 41 MS patients and 41 age- and sex-matched healthy participants received rs-fMRI, from which measures of cerebral hemodynamics and oxygenation were extracted and compared across brain regions and study groups using within- and between-group nonparametric tests, linear mixed models, and robust multiple linear regression. We found longer blood arrival times and lower blood volumes in lesions than in normal-appearing WM. Higher blood volumes were found in MS patients' deep WM lesions compared to healthy participants, and blood arrival time was more delayed in MS patients' deep WM lesions than in healthy participants. Delayed blood arrival time in the cortical grey matter was associated with greater cognitive impairment in MS patients. Perfusion imaging using rs-fMRI is useful for WM lesion characterization. rs-fMRI-based blood arrival times and volumes are associated with cognitive function.

1 | Introduction

White matter (WM) lesions that are hyperintense on T2-weighted and fluid-attenuated inversion recovery (FLAIR) sequences are common findings on brain magnetic resonance imaging (MRI) (Fazekas 1989). The most common cause of these lesions is cerebral microangiopathy, the incidence of which increases with age (Smith et al. 2017). Pathophysiologically, the manifestations of cerebral microangiopathy involve arteriolar wall thickening and lumen narrowing (Wardlaw, Benveniste, and Williams 2022; Wardlaw, Smith, and Dichgans 2019) as well as vascular and systemic inflammation (Li et al. 2020; Low et al. 2019).

Summary

- Resting-state functional MRI (rs-fMRI) can detect perfusion changes in multiple sclerosis and microangiopathic white matter lesions without contrast agents.
- Hemodynamic parameters derived from rs-fMRI differ between demyelinating and microangiopathic lesions.
- rs-fMRI-derived blood arrival time in the cortical grey matter is associated with cognitive function in multiple sclerosis.

WM lesions also occur in chronic-inflammatory central nervous system disorders like multiple sclerosis (MS). The pathological hallmark of MS is the presence of demyelinating lesions in the white and grey matter of the central nervous system (Filippi et al. 2019). The demyelinating process involves neuroinflammation with lymphocyte infiltration, microglial activation, and blood–brain barrier breakdown (Filippi et al. 2018). Microvascular occlusion with resulting ischemia also contributes to tissue damage in demyelinating lesions (Putnam 1933, 1937). Features of age-related microangiopathy are also seen in MS and likely contribute to disability in these patients (Geraldes et al. 2017). Perfusion imaging plays an important role in investigating the pathophysiology of MS (D'haeseleer et al. 2011; Lapointe et al. 2018). Acute demyelinating lesions show elevated cerebral blood flow (CBF) and cerebral blood volume (CBV) that gradually decline over time (Wuerfel et al. 2004). Reduced grey matter perfusion also correlates with cognitive impairment and disease severity in MS (Hojjat et al. 2016; Jakimovski et al. 2020).

Most studies investigating perfusion in MS have used dynamic susceptibility contrast MRI (DSC-MRI), which requires exogenous gadolinium-based contrast agents. However, the routine application of contrast agents is discouraged due to concerns about gadolinium deposition in the brain with repeated use (Brisset et al. 2020; Schlemm et al. 2017; Zivadinov et al. 2019). In addition, DSC-MRI assumes an intact blood–brain barrier (Donahue et al. 2000; Østergaard et al. 1996), which is often not the case in acute MS lesions (Filippi et al. 2018).

For these reasons, we aim to explore alternative methods for assessing cerebral perfusion. Blood arrival times can be calculated based on the systemic low-frequency oscillations in the blood-oxygenation-level-dependent (BOLD) signal in different brain regions compared with a reference region (Khalil et al. 2017). This method relies on a resting-state functional MRI (rs-fMRI) scan, does not require an exogenous contrast agent, and has been validated in several clinical contexts, including in patients with cerebrovascular diseases (Amemiya, Takao, and Abe 2023; Tong, Hocke, and Frederick 2019).

Here, we explore the differences in cerebral hemodynamic metrics derived from rs-fMRI, specifically BOLD delay (Khalil et al. 2017), oxygen level estimates (Chien et al. 2024), and BOLD coefficient of variation (CoV), a parameter related to cerebral blood volume (Khalil et al. 2017), between patients with MS and healthy participants. We hypothesized that there would be a detectable difference in rs-fMRI-extracted hemodynamic metrics between MS patients and healthy participants, particularly in brain lesions. Lesions profiled include microangiopathic and demyelinating lesions in different locations (i.e., periventricular versus deep WM). Associations between hemodynamic measures and disease severity as well as cognitive impairment in MS patients were also investigated.

2 | Material and Methods

2.1 | Study Cohort

Patient data were collected retrospectively from an ongoing, longitudinal observational MS study at the Neuroscience Clinical Research Center (NCRC), Charité-Universitätsmedizin Berlin (Cohort Study of Clinically Isolated Syndrome and Early Multiple Sclerosis, ClinicalTrials.gov Identifier: NCT01371071, start date: January 2011). Patients were included who were over the age of 18 years with a diagnosis of clinically isolated syndrome (CIS) or relapsing–remitting MS (RRMS) according to the McDonald 2017 diagnostic criteria (Thompson et al. 2018). The exclusion criteria were contraindications to MRI, other neurological diseases, or missing rs-fMRI data. Forty-one MS patients fulfilled the inclusion criteria.

We retrospectively selected 41 age- and sex-matched individuals without known neurological illnesses from a longitudinal observational cohort recruited between June 2015 and March 2019 at the NCRC. This study was approved by the local ethics committee of the Charité-Universitätsmedizin Berlin (EA1/182/10 and EA1/163/12) and conducted per the Declaration of Helsinki and German law. All patients and participants provided written informed consent.

2.2 | Clinical Measures

To evaluate clinical disability, we used the Expanded Disability Status Scale (EDSS) (Kurtzke 2015), which trained physicians collected. Cognitive dysfunction was assessed by the Symbol Digits Modalities Tests (SDMT) (Strober et al. 2020), which captures information regarding cognitive processing speed and working memory, particularly in MS patients.

2.3 | Magnetic Resonance Imaging (MRI) Acquisition

All imaging was performed on a 3 T Siemens TimTrio MRI scanner. The imaging protocol included a 3D fluid-attenuated inversion recovery (FLAIR) sequence (repetition time [TR] = 5000 ms, echo time [TE] = 388 ms, inversion time [TI] = 1800 ms, flip angle [FA] = 120, voxel size = 0.49 × 0.49 × 1.00 mm), a 3D T1-weighted magnetization prepared rapid gradient echo (T1-MPRAGE) sequence (TR = 1900 ms, TE = 2.55 ms, TI = 900 ms, FA = 9, voxel size = 0.94 × 0.94 × 1.00 mm), and a resting-state functional MRI (rs-fMRI) sequence (TR = 2250 ms, TE = 30 ms, FA = 90, voxel size = 3.4 × 3.4 × 3.4 mm, 260 volumes, total acquisition time = 585 s).

2.4 | Lesion Segmentation

All T1-MPRAGE and FLAIR images were cropped using the FMRIB Software Library's (FSL, version 5.0.9) *standard_space_roi* function, bias-corrected using ANTs' *N4BiasFieldCorrection*, and coregistered to Montreal Neurological Institute (MNI)-space 152. FLAIRs were linearly coregistered to T1-MPRAGEs using the FMRIB's Linear Image Registration Tool (FLIRT) (Jenkinson et al. 2002; Jenkinson and Smith 2001). Two expert MRI technicians with over 10 years of MS research experience manually segmented WM lesions on coregistered FLAIR images using ITK-SNAP (Yushkevich et al. 2006) (www.itksnap.org) to create binary masks (Chien et al. 2022).

2.5 | Image Processing

2.5.1 | Parcellation of Regions of Interest

The T1-MPRAGEs were lesion-filled using FSL's *lesion_filling* function (Battaglini, Jenkinson, and De Stefano 2012), and brain extraction was performed along with WM, grey matter, and cerebrospinal fluid (CSF) parcellation using the Computational Anatomy Toolbox (CAT12) version 1742 (Gaser et al. 2024). The deep grey matter masks, including the brainstem, were created using FSL FIRST (Patenaude et al. 2011).

We used FSL's Brain Intensity AbNormality Classification Algorithm (BIANCA) (Griffanti et al. 2016) to create individual masks of the lateral ventricles from the lesion-filled T1-MPRAGEs, which were dilated by 15 voxels (1 mm^3 per voxel) from the center of the mask using *fsltools* to create periventricular region masks.

To create the periventricular normal-appearing white matter (NAWM) masks, we subtracted the original lateral ventricle masks, whole deep grey matter masks, and periventricular lesion masks from the dilated periventricular region masks. To create the deep NAWM masks, we subtracted the dilated periventricular region masks, the lesions masks, and the cortical grey matter masks from the whole-brain WM masks. Lesions were classified as periventricular or deep WM lesions depending on which of the NAWM masks they intersected with.

2.5.2 | Resting-State Functional MRI Processing

The first four volumes of the rs-fMRI data were removed and the images were spatially realigned to the mean image followed by brain extraction, spatial smoothing with a 6 mm Gaussian kernel, despiking (using AFNI's *3dDespike*), regression of 6 motion parameters (three rigid body translations and three rotations), and bandpass temporal filtering (0.01–0.15 Hz). The mean and maximum framewise displacement, an estimate of motion from one volume to the next (Power et al. 2012), were calculated using FSL's *fsl_motion_outliers* function (with the "–fd" option).

BOLD delay maps were calculated using a reference signal from the large venous sinuses (Khalil et al. 2023; Tanrıtanır et al. 2020) and the *rapidtide* package (Frederick 2016). We used a time shift range of −5 to +5 s for the cross-correlation (Khalil et al. 2023). We normalized (BOLD $delay_{norm}$) each subject's voxelwise BOLD delay (BOLD $delay_{voxel}$) to the same subject's mean grey matter BOLD delay value (BOLD $delay_{GM}$) using the following equation:

$$\text{BOLD delay}_{\text{norm}} = \left(\text{BOLD delay}_{\text{GM}} - \text{BOLD delay}_{\text{voxel}}\right)^{*} - 1 \quad (1)$$

The multiplication by −1 was applied to maintain the convention that positive BOLD delay values indicate delayed arrival while negative BOLD delay values indicate earlier arrival of the BOLD oscillations compared to the oscillations in the venous sinuses.

The maximum cross-correlation values between each voxel and the venous sinus signal derived from *rapidtide* were squared and multiplied by 100 to get the percentage of the variability in the voxel's signal accounted for by the venous sinus signal. We refer to this metric as the "oxygen level estimate" (OLE) as it is a measure of similarity between the voxel's BOLD signal and the BOLD signal in areas with low-oxygenation venous blood (Chien et al. 2024). Effectively, it is assumed that the higher the OLE in a particular voxel, the more deoxygenated blood signal there is.

The BOLD coefficient of variation ($BOLD_{CoV}$) was calculated from the processed rs-fMRI data using AFNI's *3dTstat* ("-cvar" option). $BOLD_{CoV}$ has been found to correlate with cerebral blood volume (CBV) derived from DSC-MRI (Khalil et al. 2017). The formula for $BOLD_{CoV}$ per voxel is:

$$\text{BOLD}_{\text{CoV}} = \text{BOLD}_{\text{standard deviation}} / \text{BOLD}_{\text{mean}} \quad (2)$$

The BOLD delay, OLE, and CoV maps then underwent field map-based distortion-correction and registration to the T1-MPRAGE in MNI space using FSL FLIRT.

2.5.3 | Extracting Hemodynamic Metrics

Mean BOLD delay, OLE, and CoV metrics were extracted from periventricular and deep WM lesions, normal-appearing periventricular and deep WM, cortical grey matter, and subcortical grey matter structures using *fslstats* and *fslmaths*.

An overview of the image processing pipeline is shown in Figure 1.

2.6 | Statistical Analysis

Statistical analysis and data visualization were performed using R version 4.2.1 (R Core Team 2013). Descriptive statistics were calculated for each group (MS and healthy). Normality was tested using the Shapiro–Wilk test. Since most of our data were non-normally distributed, we used nonparametric statistical tests and *r*, a nonparametric alternative to Cohen's *d*, as an effect size measure (Cohen 1977; Fritz, Morris, and Richler 2012). We assessed differences in hemodynamic measures between

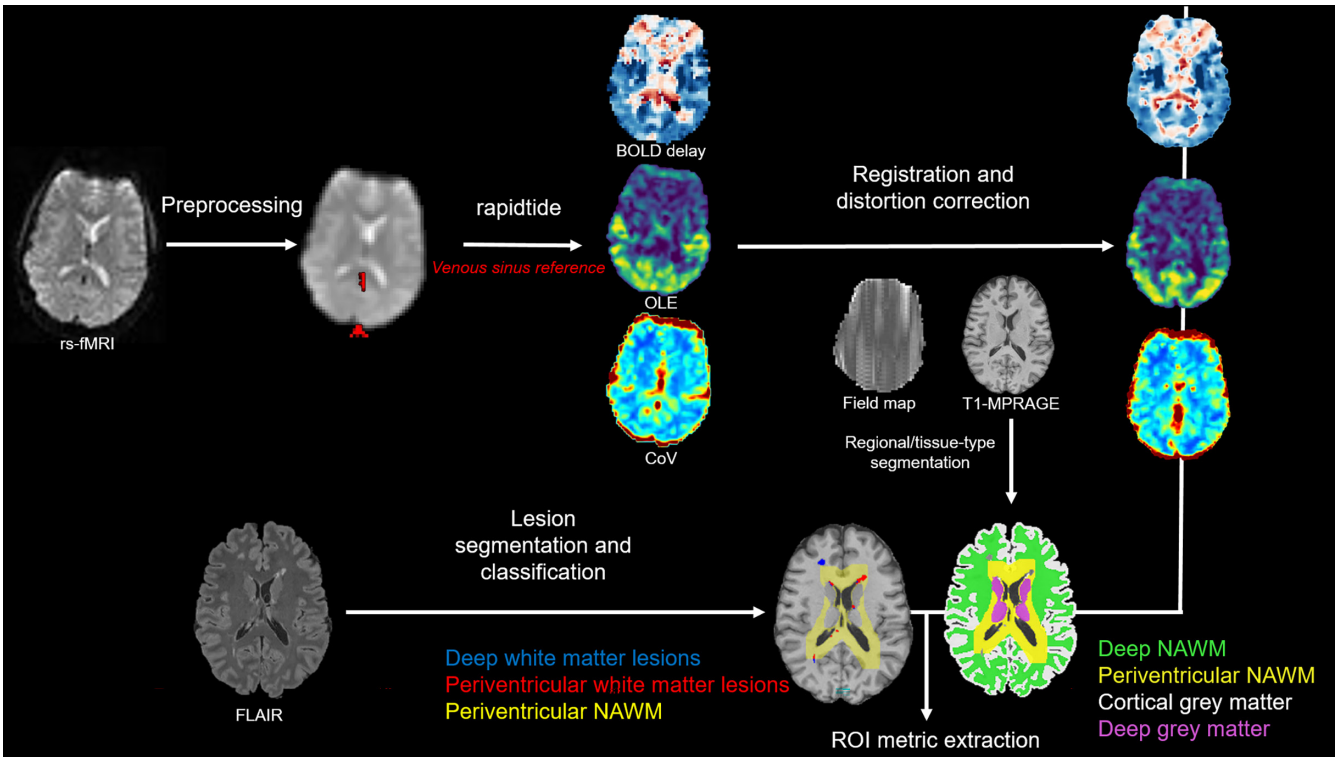

FIGURE 1 | BOLD delay, coefficient of variation (CoV), and oxygen level estimate (OLE) map creation from rs-fMRI scans and extraction of mean regional metrics. Maps were coregistered to distortion- and field-map-corrected T1-MPRAGE anatomical images where parcellated regions of periventricular normal-appearing white matter (NAWM), deep NAWM, lesions, and cortical grey matter were used to extract mean BOLD delay, CoV, and OLE from each subject.

lesion types and normal-appearing WM, between groups (MS vs. healthy), and between locations (periventricular vs. deep WM) using random intercepts linear mixed-effects models implemented using the "nlme" R package (Pinheiro J, Bates D, R Core Team 2023; Pinheiro and Bates 2000). Separate models were evaluated for BOLD delay, OLE, and CoV. Each model included subjects as the random effect. Lesion volume (mL), age (years), sex as well as the interactions between group (MS/healthy), location (periventricular/deep WM), and lesion (yes/no) were included as fixed effects.

The associations between the hemodynamic metrics and EDSS and SDMT scores were tested with robust multiple linear regression using the "lmrob" R function from the "robustbase" package (Maechler et al. 2018). Each linear regression model included age, sex, and disease duration (years) as covariates.

3 | Results

3.1 | Cohort Description

Each of the MS and healthy study groups consisted of 20 females and 21 males. Table 1 shows descriptive statistics for both groups. Figures S1 and S2 show the distribution of lesion volumes and counts in the groups, and Figure 2 shows the spatial distribution of the lesions. Figure S3 shows the mean BOLD delay and CoV maps for each of the study groups, which do not appear to differ between groups.

3.2 | Hemodynamics in WM Lesions Compared to Normal-Appearing WM

The associations between lesion volumes and lesion hemodynamic metrics are shown in Table S1. Only the association between deep NAWM CoV and lesion volume was statistically significant ($r=0.26$, $p=0.025$).

BOLD delay was higher in lesions in MS patients and healthy participants than in NAWM (Figure 3, $p<0.001$, estimate $=-0.823$). This was observed in both the periventricular region and the deep WM lesions. Periventricular lesions showed even higher BOLD delay than deep WM lesions (Table 2, interaction between location and lesion $p=0.01$, estimate $=0.581$) in both MS patients (Wilcoxon signed-rank test, $p<0.001$, $r=0.63$) and healthy participants (Wilcoxon signed-rank test, $p=0.002$, $r=0.48$).

OLE was not significantly different in either type of lesion compared to normal-appearing WM (Table 2 and Figure 4, $p=0.256$, estimate $=-1.92$) in both MS patients (Wilcoxon signed-rank test, $p=0.403$, $r=0.13$) and healthy participants (Wilcoxon signed-rank test, $p=0.847$, $r=0.03$).

CoV was lower in lesions of both MS and healthy groups than in NAWM (Table 2 and Figure 5, $p<0.001$, estimate $=0.002$). This was the case for both periventricular and deep WM lesions. Periventricular lesions showed higher CoV than deep WM lesions (Table 2, interaction between location and lesion $p=0.021$, estimate $=-0.001$) in MS patients (Wilcoxon signed-rank test,

$p = 0.002$, $r = 0.49$) but not in healthy participants (Wilcoxon signed-rank test, $p = 0.12$, $r = 0.24$).

3.3 | Hemodynamics in Lesions in MS Patients Compared to in Healthy Participants

CoV was significantly higher in periventricular (Wilcoxon rank-sum test, $p = 0.026$, $r = 0.17$) and deep WM (Wilcoxon rank-sum test, $p = 0.001$, $r = 0.25$) lesions in MS patients than in healthy participants (Figure 5).

BOLD delay was significantly higher in deep WM lesions (Wilcoxon rank-sum test, $p = 0.042$, $r = 0.16$) in MS patients than in healthy participants (Figure 3) but not in periventricular lesions (Wilcoxon rank-sum test, $p = 0.50$, $r = 0.05$).

OLE was not significantly different between MS patients and healthy participants in either periventricular (Figure 4, Wilcoxon signed-rank test, $p = 0.596$, $r = 0.04$) or deep WM lesions (Wilcoxon signed-rank test, $p = 0.963$, $r = 0$).

3.4 | Association Between Hemodynamics With Disability and Cognitive Measures in MS

The MS patients had a median EDSS of 1.5 (IQR = 1.0–2.5) and a median SDMT score of 63.5 (IQR = 53–73.5). The only statistically significant associations between the hemodynamic and cognitive measures in the MS cohort were between BOLD delay in the cortical grey matter and SDMT score (adjusted $R^2 = 0.33$, $F = 3.73$, estimate = −11.5, $t = 4.06$, $p = 0.0082$) and CoV in periventricular lesions and the EDSS (adjusted $R^2 = 0.15$,

TABLE 1 | Descriptive statistics for the study cohorts.

	Multiple sclerosis ($n = 41$)	Healthy participants ($n = 41$)
Age (years, median [IQR])	39 [34.0–43.0]	37 [30.4–43.8]
Diagnosis (CIS:RRMS)	8:33	N/A
Disease duration (months, median [IQR])	59 [59–64]	N/A
EDSS (median [IQR])	1.5 [1–2.5]	N/A
SDMT (median [IQR])	63.5 [53–73.5]	63 [56–67]
Periventricular lesion volumes (mL, median [IQR])	0.61 [0.16–1.61]	0 [0–0.03]
Periventricular lesion count (median [IQR])	12 [5–27]	0 [0–2]
Deep lesion volumes (mL, median [IQR])	0.62 [0.21–2.23]	0.02 [0–0.06]
Deep lesion count (median [IQR])	21 [7–63]	1 [0–4]
Head motion during rs-fMRI (mm, median [IQR])	0.18 [0.15–0.21]	0.16 [0.13–0.21]

Abbreviations: CIS = clinically isolated syndrome; EDSS = Expanded Disability Status Scale; IQR = interquartile range; RRMS = relapsing–remitting multiple sclerosis; rs-fMRI = resting-state functional magnetic resonance imaging; SDMT = Symbol Digit Modalities Test.

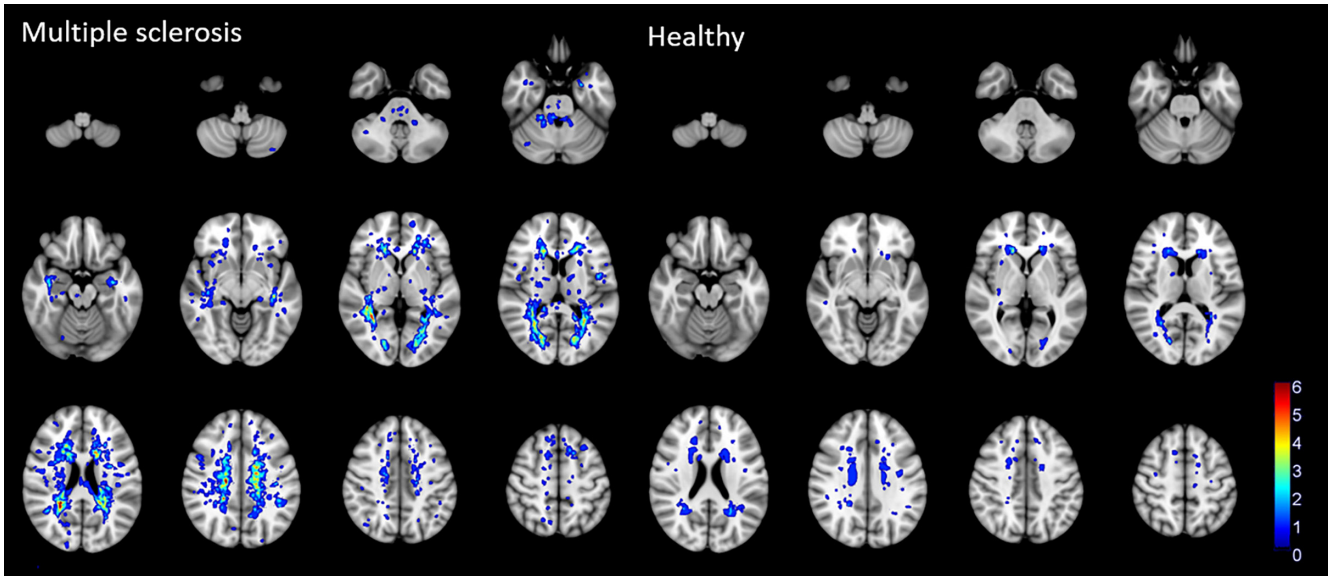

FIGURE 2 | Heat maps showing the spatial distribution of white matter lesions in multiple sclerosis patients and healthy participants.

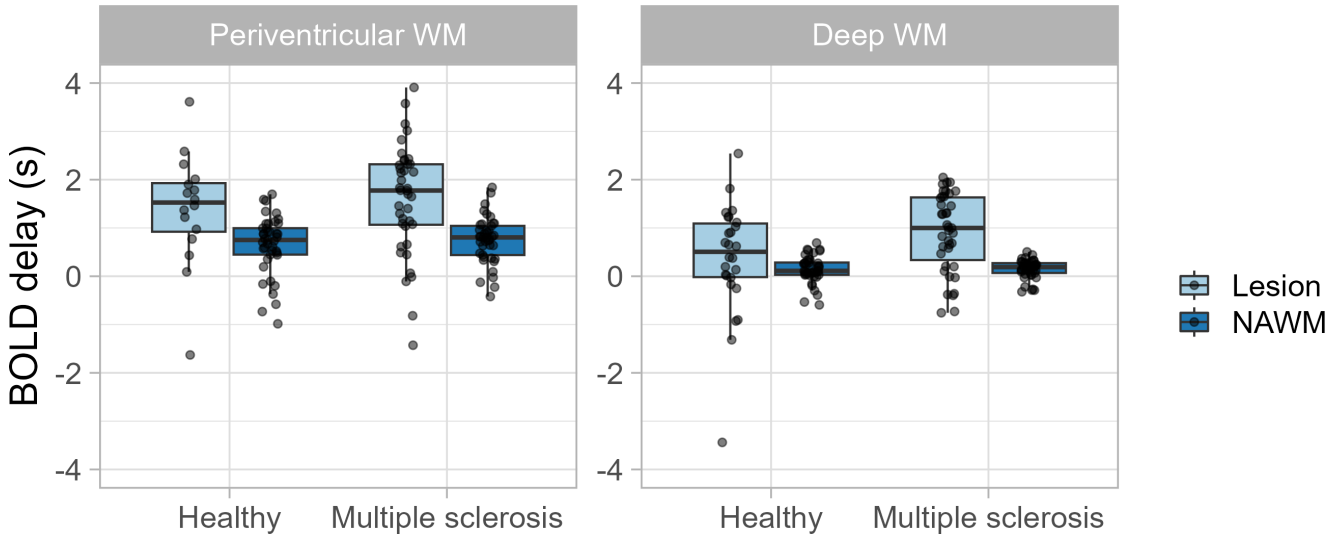

FIGURE 3 | Tukey box plots with overlain dot plots showing the distribution of BOLD delay in multiple sclerosis patients and healthy participants within white matter lesions and in normal-appearing white matter (NAWM).

$F = 1.53$, estimate $= -250.1$, $t = -2.86$, $p = 0.0071$). The rest of the results are reported in Table S2.

4 | Discussion

This study investigated cerebral hemodynamics using rs-fMRI in MS patients and healthy participants. We found that rs-fMRI-based hemodynamic measures are sensitive to differences in perfusion between WM lesions and NAWM. We also found substantial differences in some hemodynamic measures between MS and microangiopathic lesions.

Our study found a delayed blood arrival time and lower blood volume in WM lesions in both MS and healthy participants compared to the NAWM. This is consistent with previous studies showing lower CBV and longer blood arrival time in both demyelinating (Ge et al. 2005; Haselhorst et al. 2000; Ingrisch et al. 2012; Peruzzo et al. 2013; Wuerfel et al. 2004) and microangiopathic WM lesions (Dalby et al. 2019; Dewey et al. 2021; Marstrand et al. 2002; Sachdev et al. 2004).

Interestingly, we found higher blood volume in MS lesions than in microangiopathic lesions. Currently, there are no direct comparisons in the literature between CBV in demyelinating and microangiopathic WM lesions. The differences in CBV found in this study may be explained by the fact that demyelinating lesions often surround larger veins, seen on MRI as the central vein sign (Ontaneda, Cohen, and Sati 2023; Sinnecker et al. 2019). The presence of a prominent vessel results in a larger proportion of blood within a lesion, possibly explaining the higher CBV in demyelinating lesions compared to microangiopathic lesions. This study could not investigate a possible association with the central vein sign because the imaging protocol did not include susceptibility-weighted imaging.

On the other hand, blood arrival time was significantly longer in MS lesions than in microangiopathic lesions in the deep WM. The difference between the groups was not statistically significant in periventricular WM lesions. Although our exploratory study may be underpowered to detect such a difference, it is noteworthy that the physiology and hemodynamics, including venous drainage pathways, of these WM compartments are different (Okudera et al. 1999; Tabani, Tayebi Meybodi, and Benet 2020). Periventricular MS lesions are associated with high rates of lesion expansion and tissue destruction (Klistorner et al. 2022). The periventricular WM is also more sensitive to ischemia (Martinez Sosa and Smith 2017), and microangiopathic lesions in this region may thus show more severe hemodynamic disturbances than in the deep WM.

BOLD delay is sensitive to changes in venous drainage, with studies showing prolonged venous drainage times in the periventricular white matter in aging and normal pressure hydrocephalus (Aso et al. 2020; Satow et al. 2017). Inflammation and subsequent mural thickening of the small deep medullary veins that drain the periventricular white matter have been implicated in the pathogenesis of MS and microangiopathy (Adams et al. 1985; Moody et al. 1995; Sinnecker et al. 2013) and may explain the prolonged blood arrival times in periventricular MS lesions.

The susceptibility of the periventricular WM to ischemia is consistent with our finding that blood arrival time in this region is longer than in the deep WM both in lesions and NAWM of both MS patients and healthy participants. Studies using DSC-MRI and arterial spin labeling (ASL) have shown lower CBF in periventricular regions than in the rest of the WM (Dolui et al. 2019; O'Sullivan et al. 2002). Thus, our study provides further evidence that BOLD delay reflects cerebral perfusion in a way comparable to commonly used perfusion MRI techniques.

We found no association between perfusion in the cortical grey matter and MS disability severity measured using the EDSS. Some studies have found associations between grey matter perfusion and MS severity measured using the Multiple Sclerosis Severity Score (Jakimovski et al. 2020) and EDSS (de la Peña

TABLE 2 | Results of the linear mixed-effects models of the associations between hemodynamic metrics and various fixed effects.

	BOLD delay			OLE			CoV		
Predictors	**Estimate**	**CI**	***p***	**Estimate**	**CI**	***p***	**Estimate**	**CI**	***p***
(Intercept)	1.66	0.99–2.33	<0.001	16.74	6.63–26.84	0.001	0.004	0.003–0.005	<0.001
Group [MS]	0.13	−0.30 to 0.56	0.544	−3.04	−8.39 to 2.31	0.261	0.001	−0.000 to 0.001	0.092
Location [deep WM]	**−1.08**	**−1.46 to −0.71**	**<0.001**	1.74	−1.75 to 5.23	0.326	0	−0.001 to 0.000	0.123
Lesion [NAWM]	**−0.82**	**−1.18 to −0.47**	**<0.001**	−1.92	−5.25 to 1.41	0.256	**0.002**	**0.002–0.003**	**<0.001**
Lesion volume	0.01	−0.03 to 0.04	0.756	−0.16	−0.73 to 0.42	0.592	0	−0.000 to 0.000	0.578
Age	−0.01	−0.02 to 0.01	0.275	0.01	−0.22 to 0.23	0.961	0	−0.000 to 0.000	0.162
Sex [male]	0.18	−0.08 to 0.44	0.165	3.24	−0.98 to 7.46	0.131	0	−0.000 to 0.001	0.233
Group [MS] × location [deep WM]	0.39	−0.07 to 0.84	0.095	−0.17	−4.39 to 4.05	0.937	0	−0.001 to 0.001	0.952
Group [MS] × lesion [NAWM]	−0.04	−0.47 to 0.40	0.87	1.97	−2.11 to 6.04	0.342	0	−0.001 to 0.000	0.176
Location [deep WM] × lesion [NAWM]	**0.58**	**0.13–1.03**	**0.012**	2.00	−2.187 to 6.196	0.347	**−0.001**	**−0.001 to −0.000**	**0.021**
(Group [MS] × location [deep WM]) × lesion [NAWM]	−0.49	−1.07 to 0.09	0.097	1.31	−4.038 to 6.659	0.629	**0.001**	**0.000–0.002**	**0.046**

Note: The variables in square brackets indicate the reference category for the categorical variables in the models. An "x" signifies an interaction between variables in the models. Statistically significant results ($p < 0.05$) are in bold.
Abbreviations: CI = 95% confidence interval; CoV = coefficient of variation of the BOLD signal; MS = multiple sclerosis; NAWM; normal-appearing WM; OLE = oxygen level estimate; WM = white matter.

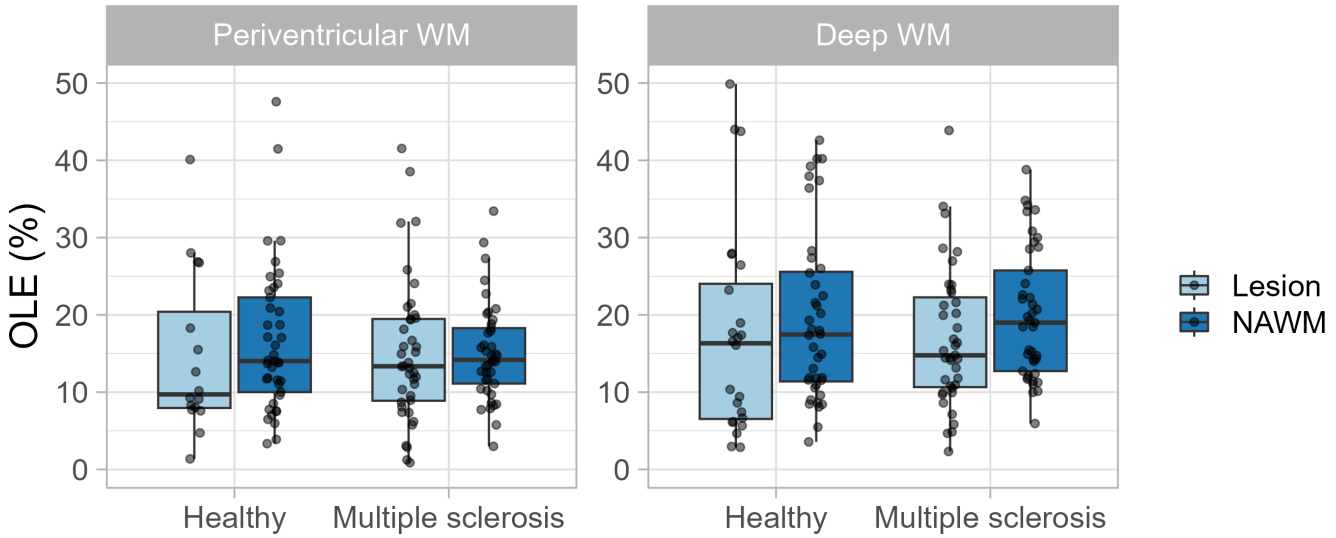

FIGURE 4 | Tukey box plots with overlain dot plots showing the distribution of oxygen level estimates in multiple sclerosis patients and healthy participants within lesions and in normal-appearing white matter (NAWM).

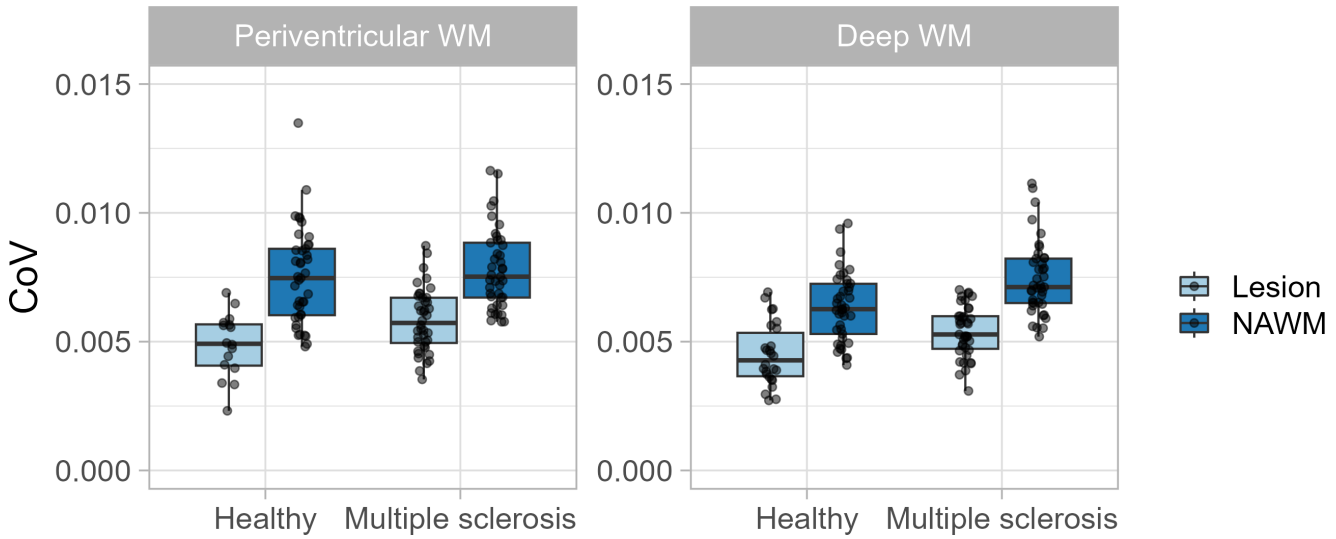

FIGURE 5 | Tukey box plots with overlain dot plots showing the distribution of coefficient of variation (CoV) in multiple sclerosis patients and healthy participants within lesions and in normal-appearing white matter (NAWM).

et al. 2019), while others have not (Debernard et al. 2014; Inglese et al. 2007). It is important to note that our study cohort had low EDSS scores, or measured disability, as most of the patients were recruited in the early stages of MS.

However, cortical grey matter blood arrival time was negatively correlated with scores on the Symbol Digit Modalities Test (SDMT), indicating that delayed perfusion in the cortical grey matter is associated with reduced attention and working memory. This is consistent with a study that found that higher CBF is associated with better executive function and attention scores in healthy individuals (Leeuwis et al. 2018). Several studies have also established a relationship between memory and cerebral perfusion in MS. Grey matter mean blood transit time measured using DSC-MRI was slightly longer in RRMS patients with cognitive impairment compared to those without (Hojjat et al. 2016). CBF measured using ASL was also negatively associated with memory test scores in a study of RRMS patients (Debernard et al. 2014). In addition, SDMT was negatively associated with total lesion volume and positively associated with grey matter CBV measured using DSC-MRI (Jakimovski et al. 2020).

The current study has several limitations. The delay in the systemic low-frequency BOLD signal oscillations between the grey matter and venous sinuses may be influenced by factors not investigated in our study, including vessel stenosis and caffeine intake (Wu et al. 2017; Yang et al. 2018). White matter lesions may also increase vascular resistance leading to prolonged blood transit times along the vascular tree (Black, Gao, and Bilbao 2009; Moody et al. 1997). Moreover, the MRI protocol did not include contrast-enhanced sequences. We were therefore

not able to distinguish between active versus chronic MS lesions. Active and chronic MS lesions differ in terms of their perfusion, with the former showing higher CBV and CBF (Ge et al. 2005; Haselhorst et al. 2000; Ingrisch et al. 2012; Wuerfel et al. 2004). The differences in hemodynamic metrics derived from rs-fMRI between active and chronic MS lesions would be interesting to investigate in the future, especially since, unlike DSC-MRI, BOLD delay does not suffer from the problem of contrast agent leakage when blood–brain barrier function is disturbed (Donahue et al. 2000; Østergaard et al. 1996). We make an implicit distinction between demyelinating and microangiopathic lesions, where there is considerable overlap between the pathophysiology of MS and microangiopathy (Li et al. 2020; Low et al. 2019; Putnam 1933, 1937). MS patients likely accumulate microangiopathic lesions over time, like healthy individuals (Geraldes et al. 2017), and both ischemic and inflammatory processes lead to WM damage in MS (Filippi et al. 2018). Although we included all brain lesions in the analysis of MS patients, our study's careful age- and sex-matching resulted in group differences likely driven by differences in pathophysiology between lesions in MS (i.e., demyelination) and healthy participants (i.e., age-related microangiopathy). Our findings should be tested in future studies with older individuals or individuals with more vascular risk factors, as the lesions in the healthy participants from our study were very small.

5 | Conclusion

Perfusion changes in MS-related and age-related WM lesions can be measured without contrast agents using resting-state fMRI. Perfusion assessment using fMRI may thus offer a convenient disease-monitoring alternative to contrast-based methods such as DSC-MRI and is a possible imaging marker for cognitive disability progression in MS. Furthermore, cerebral blood volume is significantly lower in MS lesions than in healthy participants, suggesting that it may be a useful distinguishing pathophysiological marker between WM lesions of different etiologies.

Author Contributions

A.K.: Conceptualization, Methodology, Software, Validation, Formal analysis, Data Curation, Writing – Original Draft, Writing – Review and Editing, Visualization. S.A.: Data Curation, Writing – Review and Editing. R.R.: Data Curation, Writing – Review and Editing. T.S-H.: Data Curation, Writing – Review and Editing, Resources. J.B.F.: Supervision, Resources, Funding acquisition, Writing – Review and Editing. F.P.: Data Curation, Writing – Review and Editing, Resources. C.C.: Conceptualization, Methodology, Software, Validation, Formal analysis, Data Curation, Writing – Review and Editing, Visualization, Resources.

Acknowledgments

The authors thank the members of the Time Delay Processing Group (Lia Hocke, Blaise Frederick, Ben Inglis, Ioannis Pappas, and Yunjie Tong) for their valuable input. We also thank Susan Pikol and Cynthia Kraut for their manual lesion segmentations, the Berlin Center for Advanced Neuroimaging (BCAN), and the Neuroscience Clinical Research Center (NCRC) for their administrative support. Open Access funding enabled and organized by Projekt DEAL.

Ethics Statement

This study was approved by the local ethics committee of the Charité-Universitätsmedizin Berlin (EA1/182/10 and EA1/163/12) and conducted per the Declaration of Helsinki and German law. All patients and participants provided written informed consent.

Conflicts of Interest

A.K. has received consulting fees from Bayer unrelated to this study. S.A. has received research funding from Novartis unrelated to this study and speaker's honoraria from Alexion, Bayer, and Roche. R. R. has received speaker's honoraria from Roche unrelated to this manuscript. J.B.F. has received consulting and advisory board fees from AbbVie, AC Immune, Alzheon, Artemida, BioClinica/Clario, Biogen, Bristol Myers Squibb, Brainomix, Cerevast, C2N Diagnostics, Daiichi-Sankyo, EISAI, Eli Lilly, F.Hoffmann-LaRoche AG, Forma Therapeutics, GlaxoSmithKline, Guerbet, Ionis Pharmaceuticals, IQVIA, Janssen, Julius Clinical, jung diagnostics, Lantheus Medical Imaging, Merck, Novo Nordisk, Octapharma AG, Premier Research, ProPharma Group, Prothena Biosciences, Regeneron Pharmaceuticals, Roche, Syneos, Tau Rx, Vertex Pharmaceuticals, and Worldwide Clinical Trials, outside the submitted work. F.P. has received speaker's honoraria from Alexion, Almirall, Bayer, Biogen, Roche, GlaxoSmithKline, Hexal, Merck, Sanofi, Novartis, Viela Bio, UCB, Mitsubishi, Celgene, Guthy Jackson foundation and Serono and has received research funding from DFG, BMBF and the EU unrelated to this study. C.C. has received writing honoraria from the British Society for Immunology, research funding from Novartis and Alexion unrelated to this study, and is part of a research consortium funded by the U.S. Department of Defense and is a Standing Committee on Science Member of the Canadian Institutes of Health Research (CIHR).

Data Availability Statement

The numerical data and code from this study are available from the corresponding author on request.

References

Adams, C. W., R. N. Poston, S. J. Buk, Y. S. Sidhu, and H. Vipond. 1985. "Inflammatory Vasculitis in Multiple Sclerosis." *Journal of the Neurological Sciences* 69, no. 3: 269–283. https://doi.org/10.1016/0022-510x(85)90139-x.

Amemiya, S., H. Takao, and O. Abe. 2023. "Resting-State fMRI: Emerging Concepts for Future Clinical Application." *Journal of Magnetic Resonance Imaging: JMRI* 59: 1135–1148. https://doi.org/10.1002/jmri.28894.

Aso, T., G. Sugihara, T. Murai, et al. 2020. "A Venous Mechanism of Ventriculomegaly Shared Between Traumatic Brain Injury and Normal Ageing." *Brain: A Journal of Neurology* 143, no. 6: 1843–1856. https://doi.org/10.1093/brain/awaa125.

Battaglini, M., M. Jenkinson, and N. De Stefano. 2012. "Evaluating and Reducing the Impact of White Matter Lesions on Brain Volume Measurements." *Human Brain Mapping* 33, no. 9: 2062–2071. https://doi.org/10.1002/hbm.21344.

Black, S., F. Gao, and J. Bilbao. 2009. "Understanding White Matter Disease: Imaging-Pathological Correlations in Vascular Cognitive Impairment: Imaging-Pathological Correlations in Vascular Cognitive Impairment." *Stroke; A Journal of Cerebral Circulation* 40, no. 3 Suppl: S48–S52. https://doi.org/10.1161/STROKEAHA.108.537704.

Brisset, J.-C., S. Kremer, S. Hannoun, et al. 2020. "New OFSEP Recommendations for MRI Assessment of Multiple Sclerosis Patients: Special Consideration for Gadolinium Deposition and Frequent

Acquisitions." *Journal of Neuroradiology* 47, no. 4: 250–258. https://doi.org/10.1016/j.neurad.2020.01.083.

Chien, C., J. Heine, A. Khalil, et al. 2024. "Altered Brain Perfusion and Oxygen Levels Relate to Sleepiness and Attention in Post-COVID Syndrome." *Annals of Clinical Translational Neurology* 11: 2016–2029. https://doi.org/10.1002/acn3.52121.

Chien, C., M. Seiler, F. Eitel, T. Schmitz-Hübsch, F. Paul, and K. Ritter. 2022. "Prediction of High and Low Disease Activity in Early MS Patients Using Multiple Kernel Learning Identifies Importance of Lateral Ventricle Intensity." *Multiple Sclerosis Journal - Experimental, Translational and Clinical* 8, no. 3: 20552173221109770. https://doi.org/10.1177/20552173221109770.

Cohen, J. 1977. *Statistical Power Analysis for the Behavioral Sciences*, 474. New York, NY: Academic Press.

Dalby, R. B., S. F. Eskildsen, P. Videbech, et al. 2019. "Oxygenation Differs Among White Matter Hyperintensities, Intersected Fiber Tracts and Unaffected White Matter." *Brain Communications* 1, no. 1: fcz033. https://doi.org/10.1093/braincomms/fcz033.

de la Peña, M. J., I. C. Peña, P. G.-P. García, et al. 2019. "Early Perfusion Changes in Multiple Sclerosis Patients as Assessed by MRI Using Arterial Spin Labeling." *Acta Radiologica Open* 8, no. 12: 2058460119894214. https://doi.org/10.1177/2058460119894214.

Debernard, L., T. R. Melzer, S. Van Stockum, et al. 2014. "Reduced Grey Matter Perfusion Without Volume Loss in Early Relapsing-Remitting Multiple Sclerosis." *Journal of Neurology, Neurosurgery, and Psychiatry* 85, no. 5: 544–551. https://doi.org/10.1136/jnnp-2013-305612.

Dewey, B. E., X. Xu, L. Knutsson, et al. 2021. "MTT and Blood-Brain Barrier Disruption Within Asymptomatic Vascular WM Lesions." *American Journal of Neuroradiology* 42, no. 8: 1396–1402. https://doi.org/10.3174/ajnr.A7165.

D'haeseleer, M., M. Cambron, L. Vanopdenbosch, and J. De Keyser. 2011. "Vascular Aspects of Multiple Sclerosis." *Lancet Neurology* 10, no. 7: 657–666. https://doi.org/10.1016/S1474-4422(11)70105-3.

Dolui, S., D. Tisdall, M. Vidorreta, et al. 2019. "Characterizing a Perfusion-Based Periventricular Small Vessel Region of Interest." *NeuroImage. Clinical* 23: 101897. https://doi.org/10.1016/j.nicl.2019.101897.

Donahue, K. M., H. G. Krouwer, S. D. Rand, et al. 2000. "Utility of Simultaneously Acquired Gradient-Echo and Spin-Echo Cerebral Blood Volume and Morphology Maps in Brain Tumor Patients." *Magnetic Resonance in Medicine: Official Journal of the Society of Magnetic Resonance in Medicine/Society of Magnetic Resonance in Medicine* 43, no. 6: 845–853. https://doi.org/10.1002/1522-2594(200006)43:6<845::aid-mrm10>3.0.co;2-j.

Fazekas, F. 1989. "Magnetic Resonance Signal Abnormalities in Asymptomatic Individuals: Their Incidence and Functional Correlates." *European Neurology* 29, no. 3: 164–168. https://doi.org/10.1159/000116401.

Filippi, M., A. Bar-Or, F. Piehl, et al. 2018. "Multiple sclerosis." *Nature Reviews. Disease Primers* 4, no. 1: 43. https://doi.org/10.1038/s41572-018-0041-4.

Filippi, M., P. Preziosa, B. L. Banwell, et al. 2019. "Assessment of Lesions on Magnetic Resonance Imaging in Multiple Sclerosis: Practical Guidelines." *Brain: A Journal of Neurology* 142, no. 7: 1858–1875. https://doi.org/10.1093/brain/awz144.

Frederick, B. 2016. "rapidtide (Version 0.1.8)." https://github.com/bbfrederick/rapidtide.

Fritz, C. O., P. E. Morris, and J. J. Richler. 2012. "Effect Size Estimates: Current Use, Calculations, and Interpretation." *Journal of Experimental Psychology. General* 141, no. 1: 2–18. https://doi.org/10.1037/a0024338.

Gaser, C., R. Dahnke, P. M. Thompson, F. Kurth, E. Luders, and Alzheimer's Disease Neuroimaging Initiative. 2024. "CAT – A Computational Anatomy Toolbox for the Analysis of Structural MRI Data." *GigaScience* 13: giae049. https://doi.org/10.1093/gigascience/giae049.

Ge, Y., M. Law, G. Johnson, et al. 2005. "Dynamic Susceptibility Contrast Perfusion MR Imaging of Multiple Sclerosis Lesions: Characterizing Hemodynamic Impairment and Inflammatory Activity." *AJNR. American Journal of Neuroradiology* 26, no. 6: 1539–1547.

Geraldes, R., M. M. Esiri, G. C. DeLuca, and J. Palace. 2017. "Age-Related Small Vessel Disease: A Potential Contributor to Neurodegeneration in Multiple Sclerosis." *Brain Pathology* 27, no. 6: 707–722. https://doi.org/10.1111/bpa.12460.

Griffanti, L., G. Zamboni, A. Khan, et al. 2016. "BIANCA (Brain Intensity AbNormality Classification Algorithm): A New Tool for Automated Segmentation of White Matter Hyperintensities." *NeuroImage* 141: 191–205. https://doi.org/10.1016/j.neuroimage.2016.07.018.

Haselhorst, R., L. Kappos, D. Bilecen, et al. 2000. "Dynamic Susceptibility Contrast MR Imaging of Plaque Development in Multiple Sclerosis: Application of an Extended Blood-Brain Barrier Leakage Correction." *Journal of Magnetic Resonance Imaging: JMRI* 11, no. 5: 495–505. https://doi.org/10.1002/(sici)1522-2586(200005)11:5<495::aid-jmri5>3.0.co;2-s.

Hojjat, S.-P., M. Kincal, R. Vitorino, et al. 2016. "Cortical Perfusion Alteration in Normal-Appearing Gray Matter Is Most Sensitive to Disease Progression in Relapsing-Remitting Multiple Sclerosis." *American Journal of Neuroradiology* 37, no. 8: 1454–1461. https://doi.org/10.3174/ajnr.A4737.

Inglese, M., S.-J. Park, G. Johnson, et al. 2007. "Deep Gray Matter Perfusion in Multiple Sclerosis: Dynamic Susceptibility Contrast Perfusion Magnetic Resonance Imaging at 3 T." *Archives of Neurology* 64, no. 2: 196–202. https://doi.org/10.1001/archneur.64.2.196.

Ingrisch, M., S. Sourbron, D. Morhard, et al. 2012. "Quantification of Perfusion and Permeability in Multiple Sclerosis: Dynamic Contrast-Enhanced MRI in 3D at 3T." *Investigative Radiology* 47, no. 4: 252–258. https://doi.org/10.1097/RLI.0b013e31823bfc97.

Jakimovski, D., N. Bergsland, M. G. Dwyer, et al. 2020. "Cortical and Deep Gray Matter Perfusion Associations With Physical and Cognitive Performance in Multiple Sclerosis Patients." *Frontiers in Neurology* 11: 700. https://doi.org/10.3389/fneur.2020.00700.

Jenkinson, M., P. Bannister, M. Brady, and S. Smith. 2002. "Improved Optimisation for the Robust and Accurate Linear Registration and Motion Correction of Brain Images." *NeuroImage* 17, no. 2: 825–841. https://doi.org/10.1016/S1053-8119(02)91132-8.

Jenkinson, M., and S. Smith. 2001. "A Global Optimisation Method for Robust Affine Registration of Brain Images." *Medical Image Analysis* 5, no. 2: 143–156. https://doi.org/10.1016/s1361-8415(01)00036-6.

Khalil, A. A., A.-C. Ostwaldt, T. Nierhaus, et al. 2017. "Relationship Between Changes in the Temporal Dynamics of the Blood-Oxygen-Level-Dependent Signal and Hypoperfusion in Acute Ischemic Stroke." *Stroke; A Journal of Cerebral Circulation* 48, no. 4: 925–931. https://doi.org/10.1161/STROKEAHA.116.015566.

Khalil, A. A., A. C. Tanritanir, U. Grittner, et al. 2023. "Reproducibility of Cerebral Perfusion Measurements Using BOLD Delay." *Human Brain Mapping* 44, no. 7: 2778–2789. https://doi.org/10.1002/hbm.26244.

Klistorner, S., M. H. Barnett, S. L. Graham, C. Wang, and A. Klistorner. 2022. "The Expansion and Severity of Chronic MS Lesions Follows a Periventricular Gradient." *Multiple Sclerosis* 28, no. 10: 1504–1514. https://doi.org/10.1177/13524585221080667.

Kurtzke, J. F. 2015. "On the Origin of EDSS." *Multiple Sclerosis and Related Disorders* 4, no. 2: 95–103. https://doi.org/10.1016/j.msard.2015.02.003.

Lapointe, E., D. K. B. Li, A. L. Traboulsee, and A. Rauscher. 2018. "What Have We Learned From Perfusion MRI in Multiple Sclerosis?"

AJNR. American Journal of Neuroradiology 39, no. 6: 994–1000. https://doi.org/10.3174/ajnr.A5504.

Leeuwis, A. E., L. A. Smith, A. Melbourne, et al. 2018. "Cerebral Blood Flow and Cognitive Functioning in a Community-Based, Multi-Ethnic Cohort: The SABRE Study." *Frontiers in Aging Neuroscience* 10: 279. https://doi.org/10.3389/fnagi.2018.00279.

Li, T., Y. Huang, W. Cai, et al. 2020. "Age-Related Cerebral Small Vessel Disease and Inflammaging." *Cell Death & Disease* 11, no. 10: 932. https://doi.org/10.1038/s41419-020-03137-x.

Low, A., E. Mak, J. B. Rowe, H. S. Markus, and J. T. O'Brien. 2019. "Inflammation and Cerebral Small Vessel Disease: A Systematic Review." *Ageing Research Reviews* 53: 100916. https://doi.org/10.1016/j.arr.2019.100916.

Maechler, M., P. Rousseeuw, C. Croux, et al. 2018. robustbase: Basic Robust Statistics R package (Version 0.93-4).

Marstrand, J. R., E. Garde, E. Rostrup, et al. 2002. "Cerebral Perfusion and Cerebrovascular Reactivity Are Reduced in White Matter Hyperintensities." *Stroke; a Journal of Cerebral Circulation* 33, no. 4: 972–976. https://doi.org/10.1161/01.str.0000012808.81667.4b.

Martinez Sosa, S., and K. J. Smith. 2017. "Understanding a Role for Hypoxia in Lesion Formation and Location in the Deep and Periventricular White Matter in Small Vessel Disease and Multiple Sclerosis." *Clinical Science* 131, no. 20: 2503–2524. https://doi.org/10.1042/CS20170981.

Moody, D. M., W. R. Brown, V. R. Challa, and R. L. Anderson. 1995. "Periventricular Venous Collagenosis: Association With Leukoaraiosis." *Radiology* 194, no. 2: 469–476. https://doi.org/10.1148/radiology.194.2.7824728.

Moody, D. M., W. R. Brown, V. R. Challa, H. S. Ghazi-Birry, and D. M. Reboussin. 1997. "Cerebral Microvascular Alterations in Aging, Leukoaraiosis, and Alzheimer's Disease." *Annals of the New York Academy of Sciences* 826, no. 1: 103–116. https://doi.org/10.1111/j.1749-6632.1997.tb48464.x.

Okudera, T., Y. P. Huang, A. Fukusumi, Y. Nakamura, J. Hatazawa, and K. Uemura. 1999. "Micro-Angiographical Studies of the Medullary Venous System of the Cerebral Hemisphere." *Neuropathology: Official Journal of the Japanese Society of Neuropathology* 19, no. 1: 93–111. https://doi.org/10.1046/j.1440-1789.1999.00215.x.

Ontaneda, D., J. A. Cohen, and P. Sati. 2023. "Incorporating the Central Vein Sign Into the Diagnostic Criteria for Multiple Sclerosis." *JAMA Neurology* 80, no. 7: 657–658. https://doi.org/10.1001/jamaneurol.2023.0717.

Østergaard, L., A. G. Sorensen, K. K. Kwong, R. M. Weisskoff, C. Gyldensted, and B. R. Rosen. 1996. "High Resolution Measurement of Cerebral Blood Flow Using Intravascular Tracer Bolus Passages. Part II: Experimental Comparison and Preliminary Results." *Magnetic Resonance in Medicine* 36, no. 5: 726–736. https://doi.org/10.1002/mrm.1910360511.

O'Sullivan, M., D. J. Lythgoe, A. C. Pereira, et al. 2002. "Patterns of Cerebral Blood Flow Reduction in Patients With Ischemic Leukoaraiosis." *Neurology* 59, no. 3: 321–326. https://doi.org/10.1212/wnl.59.3.321.

Patenaude, B., S. M. Smith, D. N. Kennedy, and M. Jenkinson. 2011. "A Bayesian Model of Shape and Appearance for Subcortical Brain Segmentation." *NeuroImage* 56, no. 3: 907–922. https://doi.org/10.1016/j.neuroimage.2011.02.046.

Peruzzo, D., M. Castellaro, M. Calabrese, et al. 2013. "Heterogeneity of Cortical Lesions in Multiple Sclerosis: An MRI Perfusion Study." *Journal of Cerebral Blood Flow and Metabolism* 33, no. 3: 457–463. https://doi.org/10.1038/jcbfm.2012.192.

Pinheiro, J., D. Bates, and R Core Team. 2023. "Linear and Nonlinear Mixed Effects Models (Version 3.1-163). Comprehensive R Archive Network (CRAN)." https://cran.r-project.org/web/packages/nlme/index.html.

Pinheiro, J. C., and D. M. Bates. 2000. *Mixed-Effects Models in S and S-PLUS*. New York: Springer. https://doi.org/10.1007/b98882.

Power, J. D., K. A. Barnes, A. Z. Snyder, B. L. Schlaggar, and S. E. Petersen. 2012. "Spurious But Systematic Correlations in Functional Connectivity MRI Networks Arise From Subject Motion." *NeuroImage* 59, no. 3: 2142–2154. https://doi.org/10.1016/j.neuroimage.2011.10.018.

Putnam, T. J. 1933. "The Pathogenesis of Multiple Sclerosis: A Possible Vascular Factor." *New England Journal of Medicine* 209, no. 16: 786–790. https://doi.org/10.1056/NEJM193310192091604.

Putnam, T. J. 1937. "Evidences of Vascular Occlusion in Multiple Sclerosis And Encephalomyelitis." *Archives of Neurology and Psychiatry* 37, no. 6: 1298–1321. https://doi.org/10.1001/archneurpsyc.1937.02260180078006.

R Core Team. 2013. *R: A Language and Environment for Statistical Computing*. Vienna, Austria: R Foundation for Statistical Computing. http://www.R-project.org/.

Sachdev, P., W. Wen, R. Shnier, and H. Brodaty. 2004. "Cerebral Blood Volume in T2-Weighted White Matter Hyperintensities Using Exogenous Contrast Based Perfusion MRI." *Journal of Neuropsychiatry and Clinical Neurosciences* 16, no. 1: 83–92. https://doi.org/10.1176/jnp.16.1.83.

Satow, T., T. Aso, S. Nishida, et al. 2017. "Alteration of Venous Drainage Route in Idiopathic Normal Pressure Hydrocephalus and Normal Aging." *Frontiers in Aging Neuroscience* 9: 387. https://doi.org/10.3389/fnagi.2017.00387.

Schlemm, L., C. Chien, J. Bellmann-Strobl, et al. 2017. "Gadopentetate But Not Gadobutrol Accumulates in the Dentate Nucleus of Multiple Sclerosis Patients." *Multiple Sclerosis* 23, no. 7: 963–972. https://doi.org/10.1177/1352458516670738.

Sinnecker, T., I. Bozin, J. Dörr, et al. 2013. "Periventricular Venous Density in Multiple Sclerosis Is Inversely Associated With T2 Lesion Count: A 7 Tesla MRI Study." *Multiple Sclerosis (Houndmills, Basingstoke, England)* 19, no. 3: 316–325. https://doi.org/10.1177/1352458512451941.

Sinnecker, T., M. A. Clarke, D. Meier, et al. 2019. "Evaluation of the Central Vein Sign as a Diagnostic Imaging Biomarker in Multiple Sclerosis." *JAMA Neurology* 76, no. 12: 1446–1456. https://doi.org/10.1001/jamaneurol.2019.2478.

Smith, E. E., G. Saposnik, G. J. Biessels, et al. 2017. "Prevention of Stroke in Patients With Silent Cerebrovascular Disease: A Scientific Statement for Healthcare Professionals From the American Heart Association/American Stroke Association." *Stroke; a Journal of Cerebral Circulation* 48, no. 2: e44–e71. https://doi.org/10.1161/STR.0000000000000116.

Strober, L. B., J. M. Bruce, P. A. Arnett, et al. 2020. "A New Look at an Old Test: Normative Data of the Symbol Digit Modalities Test -Oral Version." *Multiple Sclerosis and Related Disorders* 43: 102154. https://doi.org/10.1016/j.msard.2020.102154.

Tabani, H., A. Tayebi Meybodi, and A. Benet. 2020. "Venous Anatomy of the Supratentorial Compartment." *Handbook of Clinical Neurology* 169: 55–71. https://doi.org/10.1016/B978-0-12-804280-9.00003-2.

Tanrıtanır, A. C., K. Villringer, I. Galinovic, et al. 2020. "The Effect of Scan Length on the Assessment of BOLD Delay in Ischemic Stroke." *Frontiers in Neurology* 11: 381. https://doi.org/10.3389/fneur.2020.00381.

Thompson, A. J., B. L. Banwell, F. Barkhof, et al. 2018. "Diagnosis of Multiple Sclerosis: 2017 Revisions of the McDonald Criteria." *Lancet Neurology* 17, no. 2: 162–173. https://doi.org/10.1016/S1474-4422(17)30470-2.

Tong, Y., L. M. Hocke, and B. B. Frederick. 2019. "Low Frequency Systemic Hemodynamic "Noise" in Resting State BOLD fMRI:

Characteristics, Causes, Implications, Mitigation Strategies, and Applications." *Frontiers in Neuroscience* 13: 787. https://doi.org/10.3389/FNINS.2019.00787.

Wardlaw, J. M., H. Benveniste, and A. Williams. 2022. "Cerebral Vascular Dysfunctions Detected in Human Small Vessel Disease and Implications for Preclinical Studies." *Annual Review of Physiology* 84: 409–434. https://doi.org/10.1146/annurev-physiol-060821-014521.

Wardlaw, J. M., C. Smith, and M. Dichgans. 2019. "Small Vessel Disease: Mechanisms and Clinical Implications." *Lancet Neurology* 18, no. 7: 684–696. https://doi.org/10.1016/S1474-4422(19)30079-1.

Wu, J., S. Dehkharghani, F. Nahab, J. Allen, and D. Qiu. 2017. "The Effects of Acetazolamide on the Evaluation of Cerebral Hemodynamics and Functional Connectivity Using Blood Oxygen Level-Dependent MR Imaging in Patients With Chronic Steno-Occlusive Disease of the Anterior Circulation." *AJNR. American Journal of Neuroradiology* 38, no. 1: 139–145. https://doi.org/10.3174/ajnr.A4973.

Wuerfel, J., J. Bellmann-Strobl, P. Brunecker, et al. 2004. "Changes in Cerebral Perfusion Precede Plaque Formation in Multiple Sclerosis: A Longitudinal Perfusion MRI Study." *Brain: A Journal of Neurology* 127, no. Pt 1: 111–119. https://doi.org/10.1093/brain/awh007.

Yang, H.-C. S., Z. Liang, J. F. Yao, X. Shen, B. D. Frederick, and Y. Tong. 2018. "Vascular Effects of Caffeine Found in BOLD fMRI." *Journal of Neuroscience Research* 97: 456–466. https://doi.org/10.1002/jnr.24360.

Yushkevich, P. A., J. Piven, H. C. Hazlett, et al. 2006. "User-Guided 3D Active Contour Segmentation of Anatomical Structures: Significantly Improved Efficiency and Reliability." *NeuroImage* 31, no. 3: 1116–1128. https://doi.org/10.1016/j.neuroimage.2006.01.015.

Zivadinov, R., N. Bergsland, J. Hagemeier, et al. 2019. "Cumulative Gadodiamide Administration Leads to Brain Gadolinium Deposition in Early MS." *Neurology* 93, no. 6: e611–e623. https://doi.org/10.1212/WNL.0000000000007892.

Supporting Information

Additional supporting information can be found online in the Supporting Information section.